



Preparation, characterization and optical properties of copper oxide nanoparticles via auto-combustion method

Ayman A. Ali*, Ibrahim S. Ahmed, Alaa S. Amin and Mai M. Gneidy

Chemistry Department, Faculty of science, Benha University, Benha, Egypt

*Corresponding author: ayman.abdelrazik@fsc.bu.edu.eg

Abstract

Copper nanoparticles have been successfully synthesized by using low auto-combustion synthesis method followed by calcination at 500 °C for two hours. The calcined copper oxide nanoparticles were investigated by various tools such as XRD, DRS, FT-IR and HR-TEM. The characteristic absorption peak at 535 cm⁻¹ corresponds to copper-oxygen stretching vibration mode of copper oxide. The HR-TEM micrograph of the obtained copper oxide sample reveals the spherical nanoparticles with soft agglomeration and the average particle size calculated from TEM-image is about 35 nm for CTA sample.

Received; 13 Mars 2019, Revised form; 12 Dec. 2019, Accepted; 12 Dec. 2019, Available online 1 April 2020.

1. Introduction:

At recent days, nanomaterials are utilized in various applications due to their advanced properties. These materials characterized by high reactivity, small size, special electronic characteristic and perfect optical properties compared to the bulk materials [1]. There are different techniques for the synthesis of inorganic oxide nanoparticles like combustion [2-4], precipitation [5], green [6], hydrothermal [7], microwave [8] and sol gel methods [9]. Many inorganic oxide nanoparticles such as zinc oxide, copper oxide, titanium oxide, stannic oxide, zirconium oxide and other oxides have considered as attractive photo-catalysts because of their high catalytic activity in the decomposition of different environmental organic pollutants like pesticides, detergents, and dyes under UV and sun light irradiation [10-13]

Copper oxide is one of the transition metal oxide that classified as important semiconductor as it have narrow band gap 1.4 eV [14]. This advantage make it suitable for application of gas sensors [15], photo catalysts [16] and electrochemical sensors[17], lithium ion batteries [18]. Nanometal oxide is also used for removal various organic dyes from waste water as methylene blue dye [6, 19-21]. Methylene blue has harmful effect when exposing to it for along time that they can cause tissue narcosis, heart stroke, jaundice, etc., in humans [22, 23]. We are used low combustion synthesis method due to easy, rapid method and saves both time and energy [24, 25]. It also used to synthesis pure, homogeneous and crystalline materials. In the present work, we aimed to synthesize copper oxide nanoparticles by using auto-combustion synthesis

following by the calcination to improve the crystallinity. The structure, optical and morphology properties of the obtained copper oxide are well characterized by different tools such as XRD, FT-IR, DRS and TEM.

2. Experimental:

2.1. Materials and reagents:

All chemicals used in this work were purchased and used as received without any further purification. Copper nitrate trihydrate (Cu(NO₃)₃.3H₂O; 99 %) was purchased from Sigma-Aldrich company. Citric acid (CA: C₆H₈O₇; 99.5%) and tartaric acid (TA: C₄H₆O₆; 99 %) were obtained from El Nasr pharmaceutical chemicals company and was purchased from Sigma-Aldrich chemical company.

2.2. Preparation of copper oxide nanoparticles via auto-combustion method:

0.02 mole of copper nitrate and calculated amount of fuels were dissolved in 50 ml distilled water, separately. The ratio between the fuel and copper nitrate calculated according to the equations (No. 1 to 3) and the rule of combustion method. The obtained solutions were preheated at 120 °C on hotplate to complete and the viscous gel was produced. Then, the gels ignited at 250 °C on hotplate, producing a grey-black ash powder. The synthesized ash calcined at 500 °C for 2 hrs to remove the residual organic material and get pure copper oxide nanoparticles. Table (1) shows the composition of starting materials, fuels type and names of products after calcination.

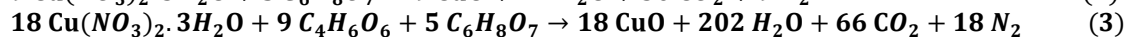
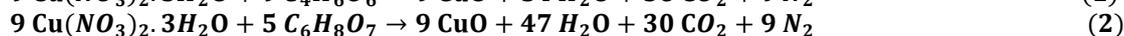
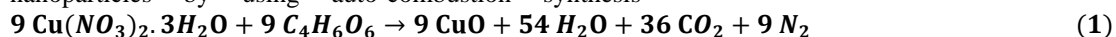


Table (1): The sample names, fuels type and the composition of the starting materials.

N	Sample names	Cu ²⁺ , mole	Type of fuel	Fuel, mole
1	CTA	0.02	TA	0.02
2	CCA	0.02	CA	0.01
3	CCTA	0.02	TA and CA	0.01+0.0055

Where: TA= tartaric acid and CA= citric acid

2.3. Characterization:

X-ray diffraction (XRD) of the calcined sample was measured using diffractometer (Bruker; model D8 advance) with monochromated Cu-K α radiation, 1.54178 (°Å) in the 2 θ range of 15-80°. FT-IR spectra were measured using FT-IR spectrometer (Bomem; model MB 157S) from 4000 to 400 cm⁻¹ at room temperature. The morphology and particle size of sample was studied using a high transmission electron microscope (HR-TEM, JEOL; model 1200 EX) at an electron voltage of 200 KV. Diffuse reflectance of calcined sample studied in ultraviolet–visible NIR range (200–2500 nm) using Jasco-V670 spectrophotometer and

integrating sphere calibrated with the white standard as barium sulfate.

3. Result and Discussion:

3.1. X-ray diffraction (XRD):

Figure (1) displays the XRD pattern of copper oxide after calcination at 500 °C for 2 hrs. There are various diffraction lines observed accord with diffraction peaks obtained by (110), (-111), (111), (-202), (020), (202), (-113), (022), (-311) and (004) planes of monoclinic symmetry of copper oxide with lattice parameters, a = 4.6837 Å, b = 3.4226 Å and c = 5.1288 Å (JCPDS Card No. 01-072-0629). Coprous oxide appeared only in case the using of citric acid fuel with 3%.

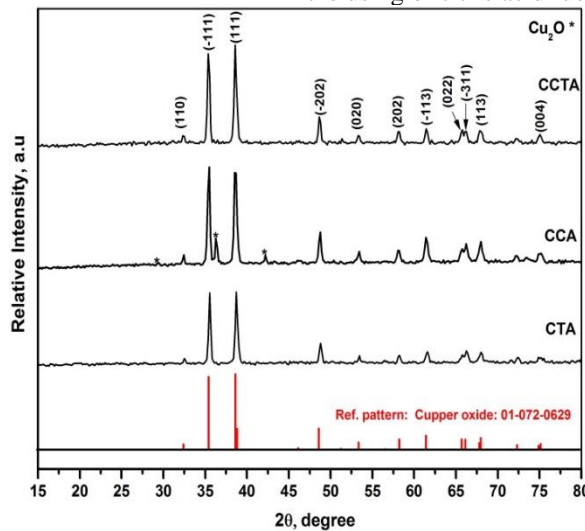


Fig (1): XRD pattern of copper oxide synthesized after calcination at 500 °C for 2 hrs

The crystal sizes (S) of the calcined samples determined using Scherrer formula in the light of the following formula (4):

$$S = 0.9\lambda / Z_{1/2} \cos \theta_B \quad (4)$$

Where, θ is the diffraction angle, λ is wavelength (0.15406 nm for Cu K α) and Z is the x-ray full width at half-maximum height (FWHM) of the diffraction peak.

The average crystallite size calculated from the x-ray diffraction lines are 40, 34 and 52 nm. Table (2, 3 and 4) summarized the position (2 θ), d values, intensity (%), crystal sizes at each peak and (hkl) values for the synthesized samples using tartaric acid, citric acid and a mixture of them, respectively.

Table (2): The extracted data from XRD pattern for the synthesized CuO using tartaric acid (CTA).

Position (2 θ)	d value (Å)	Crystal Size (nm)	Intensity %	(hkl)
32.58119	2.74495	47.5	11.4	110
35.57524	2.51924	59.5	98.6	-111
38.76688	2.32086	43.1	100	111
48.81685	1.86299	47.4	31.6	-202
53.61177	1.71112	10.8	14.8	020
58.22886	1.58277	63.3	14.5	202
61.57119	1.50367	39.9	18.8	-113
66.12771	1.40772	15.7	18.9	-311
68.01648	1.3753	32.7	16.5	113

Table (3): The extracted data from XRD pattern for the synthesized CuO using citric acid (CCA).

Position (2θ)	d value (Å)	Crystal Size (nm)	Intensity %	(hkl)
32.45283	2.75606	118.3	14.3	110
35.44945	2.528	53.9	96.5	-111
38.64929	2.32684	39.4	100	111
48.71601	1.86579	45.8	31.8	-202
53.22201	1.71337	17	12.5	020
58.15868	1.58402	38.1	16.1	202
61.47754	1.50574	57.3	17.2	-113
65.74886	1.41796	34.8	17.1	022
66.20759	1.40978	78.2	15.7	-311
67.94665	1.37808	35.8	16.7	113

Table (4): The extracted data from XRD pattern for the synthesized CuO using citric acid (CCTA).

Position (2θ)	d value (Å)	Crystal Size (nm)	Intensity %	(hkl)
32.05488	2.75055	33	12.9	110
35.52534	2.5226	56	94.2	-111
36.42687	2.4629	69	29	-
38.71097	2.32292	43.7	100	111
42.10927	2.13265	15	10.9	-
46.31381	1.95901	3.1	5.1	-112
48.80554	1.86322	47	31.5	-202
53.48454	1.71116	16	13.9	X020
58.18717	1.58331	29.8	13.2	202
61.49699	1.50519	29.2	23.9	-113
65.75463	1.41779	26.9	13.8	x022
66.28376	1.40829	44.2	18.8	-311
67.98817	1.3766	29	21.9	113

3.2. FT-IR analysis

The FT-IR spectra of the obtained copper oxide (CTA, CCA and CCTA) after calcination at 500 °C are shown in Figure 2 (a and b). The absorption peaks at 3415–3434 cm⁻¹ and 1639–1644 cm⁻¹ are indexed to the stretching and bending vibration modes of hydroxide groups of adsorbed water on the surface of the obtained copper oxide nanoparticles. The weak absorption band at 1344 cm⁻¹, 2920(5)–2840(5) cm⁻¹, 1515(7) cm⁻¹ and 1026–1035 cm⁻¹ are assigned to the nitrate, CH aliphatic, carbon-carbon

and carbon-oxygen groups, respectively. The characteristic absorption peaks at 535 cm⁻¹ indicates the stretching vibration mode of Cu-O in copper oxide nanoparticles. Also, Figure 2(b) shows the shoulder at 450(5) cm⁻¹, 480 cm⁻¹ and 580 cm⁻¹ which relate to characteristic vibrations of Cu–O bond in CuO. Only CCA sample shows the peak at 712 cm⁻¹ corresponds to the vibration of Cu-O in cuprous oxide.

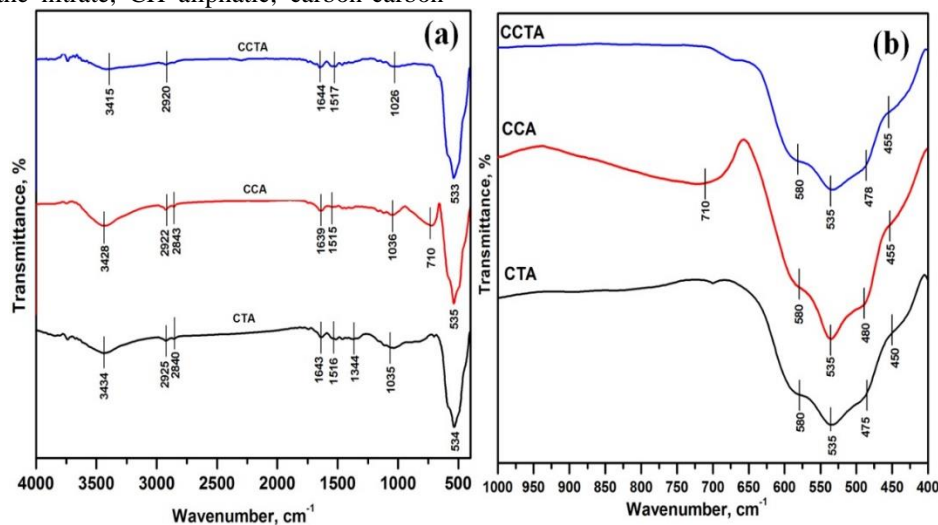


Fig (2): FTIR spectra of copper oxide synthesized after calcination at 500 °C for 2 hrs.

3.3. The morphology studies:

Figure (3) shows the morphology of CTA sample after calcination at 500 for 2 hrs. The calcined copper oxide nanoparticles were investigated by high-resolution transmission electron microscopy (HR-TEM). As shown in the HR-TEM micrograph, the morphology of the calcined copper oxide sample detects the spherical nanoparticles with soft agglomeration. The average particle size determined from TEM-image is about 35 nm for CTA sample.

3.4. Optical studies:

CTA, CCA and CCTA samples investigated using UV-Vis and NIR diffuse reflectance and absorbance spectra of the calcined copper oxides as shown in Figure 4a. Spectra show the reflectance edge between 750-800 nm for all samples. Spectra of copper oxide show the broad

absorption band between 250-800 nm with heads at 610 nm, 660 nm and 600 nm for CTA, CCA and CCTA samples, respectively as shown in figure 4(b). The band gap of the prepared powder can be determined by using the equation (5) as shown as the following:

$$(F(R)h\nu) = A(h\nu - E_g)^Y \quad (5)$$

Where, h and ν are constants, $F(R)$ is Kubelka Munk function, $F(h\nu)$ is energy function, R is the reflectance of the samples, and Y is the value between 1/2 and 2 depending on the direct and indirect allowed electronic transitions, respectively. The band gap calculated to be 1.34, 1.25 and 1.44 eV for CTA, CCA and CCTA samples, respectively as shown in Figure (5).

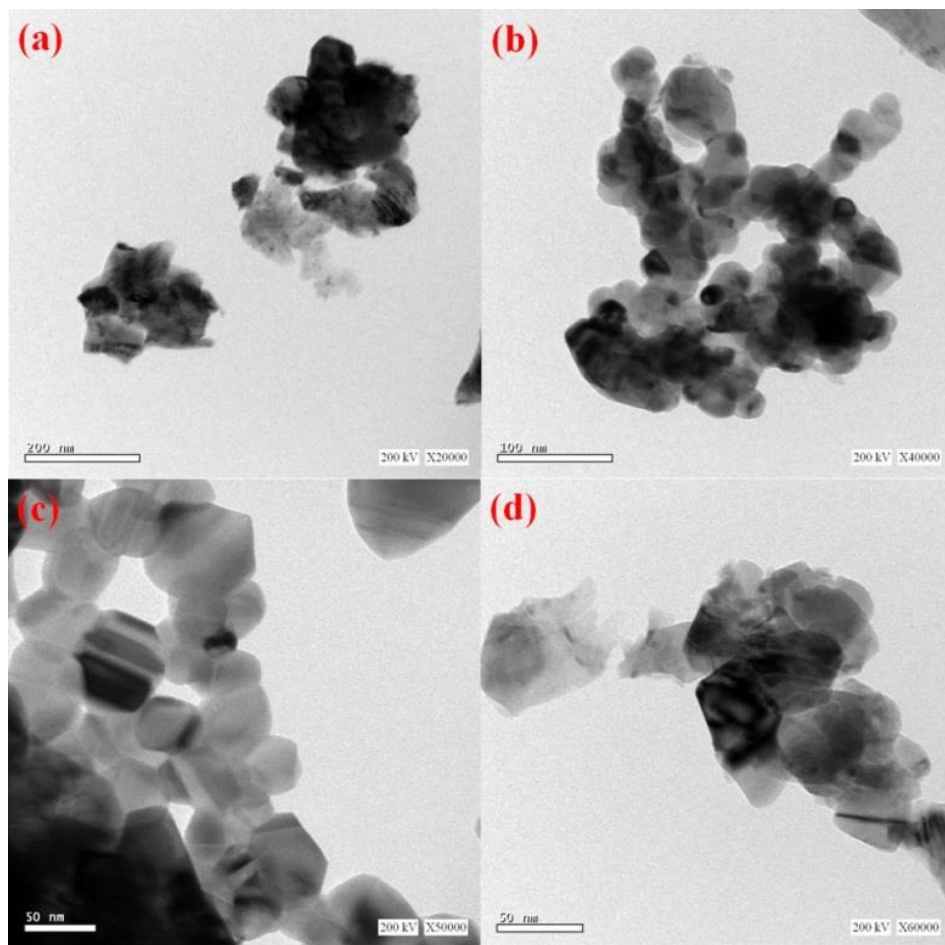


Fig (3): HRTEM of the synthesized copper oxide (CTA sample) after calcination at 500 °C for 2 hrs.

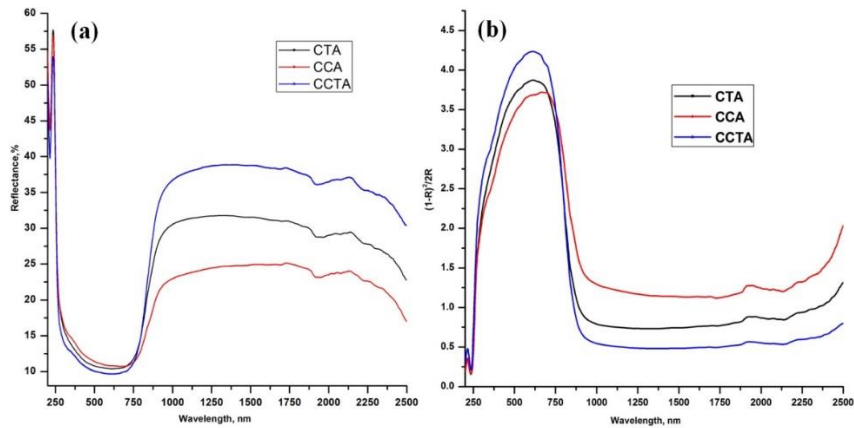


Fig (4): UV-Vis and NIR diffuse reflectance (a) and UV-vis-NIR absorption spectra (b).

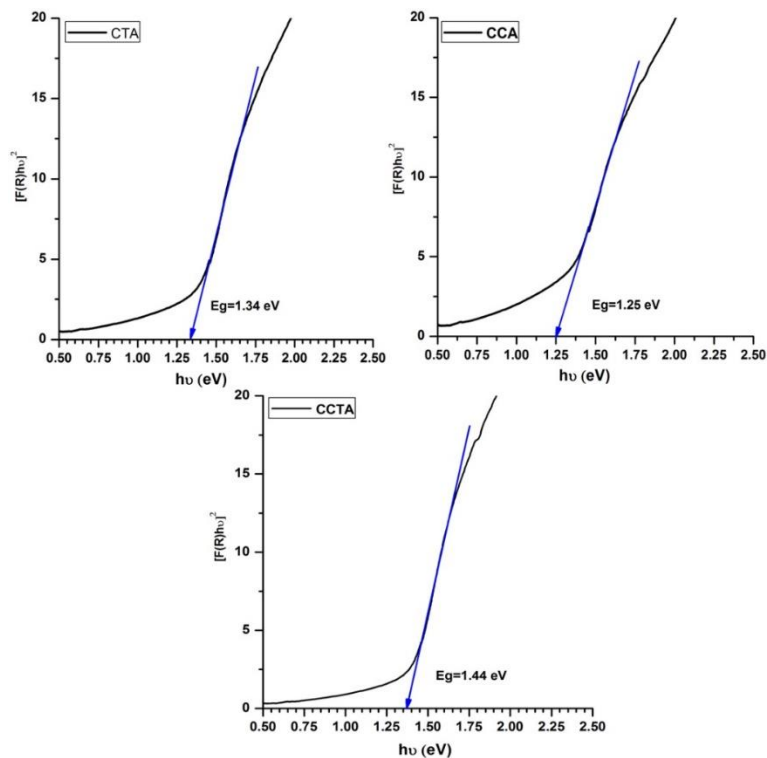


Fig (5): the band gap of the synthesized copper oxide samples after calcination at 500 °C for 2 hrs.

4. Conclusion

Copper oxide nanoparticles were fabricated from copper nitrate and organic fuel (citric acid and tartaric acid) using combustion method. The as-prepared samples were calcined at 500 °C for 2hrs and the obtained samples (CTA, CCA and CCTA) were characterized using various techniques such as x-ray powder diffraction (XRD), Fourier transform infrared analysis (FTIR) and high-

resolution transmission electron microscopy (HR-TEM). The average crystallite size of the calcined copper oxide was determined to be 40, 34 and 52 nm for CTA, CCA and CCTA samples respectively. UV-Vis-NIR diffuse reflectance spectra of calcined copper oxide show the reflectance edge at 750 nm. The band gap determined to be 1.34, 1.25 and 1.44 eV.

Acknowledgements

The authors express their thanks to Benha University, Benha, Egypt for support of the current research.

Reference

- [1] S. Meshram, P. Adhyapak, U. Mulik, D. Amalnerkar, Facile synthesis of CuO nanomorphs and their morphology dependent sunlight driven photocatalytic properties, Chemical engineering journal 204 (2012) 158-168.

- [2] A. Ali, M. Allazov, T. Ilyasli, Fabrication and study Tb^{3+} : $MgAl_2O_4$ by combustion method using malonic acid dihydrazide as fuel, *International Journal of Advanced Scientific and Technical Research* 1 (2013) 358-367.
- [3] A. Ali, E. El Fadaly, I. Ahmed, Near-infrared reflecting blue inorganic nano-pigment based on cobalt aluminate spinel via combustion synthesis method, *Dyes and Pigments* 158 (2018) 451-462.
- [4] A.A. Ali, M.R. Allazov, T.M. Ilyasli, Synthesis and characterization of magnesium aluminates spinel via combustion method using malonic acid dihydrazide as fuel, *Caspian Journal of Applied Sciences Research* 2 (2013) 85-90.
- [5] M.P. Rao, S. Anandan, S. Suresh, A.M. Asiri, J.J. Wu, Surfactant assisted synthesis of copper oxide nanoparticles for photocatalytic degradation of methylene blue in the presence of visible light, *Energy and Environment Focus* 4 (2015) 250-255.
- [6] M. Behera, G. Giri, Inquiring the photocatalytic activity of cuprous oxide nanoparticles synthesized by a green route on methylene blue dye, *International Journal of Industrial Chemistry* 7 (2016) 157-166.
- [7] M. Dar, Y. Kim, W. Kim, J. Sohn, H. Shin, Structural and magnetic properties of CuO nanoneedles synthesized by hydrothermal method, *Applied Surface Science* 254 (2008) 7477-7481.
- [8] H. Wang, J.-Z. Xu, J.-J. Zhu, H.-Y. Chen, Preparation of CuO nanoparticles by microwave irradiation, *Journal of crystal growth* 244 (2002) 88-94.
- [9] F. Wang, H. Li, Z. Yuan, Y. Sun, F. Chang, H. Deng, L. Xie, H. Li, A highly sensitive gas sensor based on CuO nanoparticles synthesized via a sol-gel method, *RSC Advances* 6 (2016) 79343-79349.
- [10] T. Chankhanittha, S. Nanan, Hydrothermal synthesis, characterization and enhanced photocatalytic performance of ZnO toward degradation of organic azo dye, *Mater. Lett.* 226 (2018) 79-82.
- [11] M. Driessen, T. Miller, V. Grassian, Photocatalytic oxidation of trichloroethylene on zinc oxide: characterization of surface-bound and gas-phase products and intermediates with FT-IR spectroscopy, *Journal of Molecular Catalysis A: Chemical* 131 (1998) 149-156.
- [12] M.R. Hoffmann, S.T. Martin, W. Choi, D.W. Bahnemann, Environmental applications of semiconductor photocatalysis, *Chem. Rev.* 95 (1995) 69-96.
- [13] R. Sankar, P. Manikandan, V. Malarvizhi, T. Fathima, K.S. Shivashangari, V. Ravikumar, *Green*
- [24] I. Ahmed, H. Dessouki, A. Ali, Synthesis and characterization of $NixMg_{1-x}Al_2O_4$ nano ceramic pigments via a combustion route, *Polyhedron* 30 (2011) 584-591.
- [25] I.S. Ahmed, S.A. Shama, H.A. Dessouki, A.A. Ali, Synthesis, thermal and spectral characterization of synthesis of colloidal copper oxide nanoparticles using Carica papaya and its application in photocatalytic dye degradation, *Spectrochimica Acta Part A: Molecular and Biomolecular Spectroscopy* 121 (2014) 746-750.
- [14] M. Vaseem, A. Umar, Y. Hahn, D. Kim, K. Lee, J. Jang, J.S. Lee, Flower-shaped CuO nanostructures: structural, photocatalytic and XANES studies, *Catalysis Communications* 10 (2008) 11-16.
- [15] A. Aslani, V. Oroojpour, CO gas sensing of CuO nanostructures, synthesized by an assisted solvothermal wet chemical route, *Physica B: Condensed Matter* 406 (2011) 144-149.
- [16] M.A. Prathap, B. Kaur, R. Srivastava, Hydrothermal synthesis of CuO micro-/nanostructures and their applications in the oxidative degradation of methylene blue and non-enzymatic sensing of glucose/ H_2O_2 , *Journal of colloid and interface science* 370 (2012) 144-154.
- [17] H.-Y. Yu, M.-Q. Xu, S.-H. Yu, G.-C. Zhao, A novel non-enzymatic glucose sensor based on CuO-graphene nanocomposites, *International Journal of Electrochemical Science* 8 (2013) 8050-8057.
- [18] J. Xiang, J. Tu, L. Zhang, Y. Zhou, X. Wang, S. Shi, Self-assembled synthesis of hierarchical nanostructured CuO with various morphologies and their application as anodes for lithium ion batteries, *Journal of Power Sources* 195 (2010) 313-319.
- [19] A. Pourahmad, Ag₂S nanoparticle encapsulated in mesoporous material nanoparticles and its application for photocatalytic degradation of dye in aqueous solution, *Superlattices and Microstructures* 52 (2012) 276-287.
- [20] M.A.M. Salleh, D.K. Mahmoud, W.A.W.A. Karim, A. Idris, Cationic and anionic dye adsorption by agricultural solid wastes: A comprehensive review, *Desalination* 280 (2011) 1-13.
- [21] K. Turhan, S.A. Ozturkcan, Decolorization and degradation of reactive dye in aqueous solution by ozonation in a semi-batch bubble column reactor, *Water, Air, & Soil Pollution* 224 (2013) 1353.
- [22] K.V. Kumar, V. Ramamurthi, S. Sivanesan, Modeling the mechanism involved during the sorption of methylene blue onto fly ash, *Journal of colloid and interface science* 284 (2005) 14-21.
- [23] M.M. Nassar, Y.H. Magdy, Removal of different basic dyes from aqueous solutions by adsorption on palm-fruit bunch particles, *Chemical Engineering Journal* 66 (1997) 223-226.
- nanosized $NixMg_{1-x}Al_2O_4$ powders as new ceramic pigments via combustion route using 3-methylpyroazole-5-one as fuel, *Spectrochimica Acta Part A: Molecular and Biomolecular Spectroscopy* 81 (2011) 324-333.